sustainability

MDPI

Article

Cyclic Fatigue Durability of Woven Geotextiles for Use in Sustainable Waste-Dewatering Systems

Mag Geisielly Alves Guimarães [1,*], Pedro Victor Garcia de Oliveira [2], Denise de Carvalho Urashima [1], Eleonardo Lucas Pereira [2] and Beatriz Mydori Carvalho Urashima [3]

[1] Post-Graduation Program in Civil Engineering, Federal Center of Technological Education of Minas Gerais (CEFET-MG), Belo Horizonte 30510-000, MG, Brazil; urashima@cefetmg.br
[2] Post-Graduation Program in Geotechnics, Federal University of Ouro Preto (NUGEO/EM/UFOP), Ouro Preto 35400-000, MG, Brazil; pedro.oliveira@alfamed.com (P.V.G.d.O.); eleonardo@ufop.edu.br (E.L.P.)
[3] Graduate School of Engineering, Osaka University, Suita 565-0871, Osaka, Japan; carvalho_b@civil.eng.osaka-u.ac.jp
* Correspondence: mag@cefetmg.br

Abstract: Geosynthetics are increasingly used in geotechnical engineering to replace conventional solutions due to their cost-effective and environmental benefits. For example, geotextiles can be used in sustainable waste-dewatering systems to confine solid waste for final disposal. This study is presented to analyze the durability of a geotextile regarding cyclic fatigue induced during the pumping stages in these sustainable waste-dewatering systems. A polypropylene woven geotextile was used and subjected to cyclic tensile loading levels of 10%, 30% and 50% of the ultimate average tensile strength. We also used hysteresis loops with a frequency of 0.1 Hz at different numbers of cycles (10, 20, 30, and 90 cycles). With a 95% confidence level and response surface, the results show that increasing the tensile loading levels and the number of cycles made the geotextile lose its tensile strength. Laboratory experiments simulated scenarios where the geotextile was subjected to cyclic fatigue that might directly impact its strength–strain and hysteretic stiffness performance over its design lifetime. This study contributes to a better understanding of the durability of geotextiles to subsidize decision-making involving social, environmental, and technical impacts in waste-dewatering system applications.

Keywords: geosynthetics; durability; sustainable; cyclic fatigue; waste-dewatering systems; geotechnical engineering

Citation: Guimarães, M.G.A.; Oliveira, P.V.G.d.; Urashima, D.d.C.; Pereira, E.L.; Urashima, B.M.C. Cyclic Fatigue Durability of Woven Geotextiles for Use in Sustainable Waste-Dewatering Systems. *Sustainability* **2023**, *15*, 13807. https://doi.org/10.3390/su151813807

Academic Editor: Alessio Siciliano

Received: 3 July 2023
Revised: 10 September 2023
Accepted: 12 September 2023
Published: 15 September 2023

1. Introduction

1.1. Initial Concepts

In the current Anthropocene era, one of the problems to solve is the final disposal of wastes generated in different industrial processes without causing environmental impacts [1]. Designing with geosynthetics has become more viable since these materials can be more efficiently produced and are more cost-effective, durable, and environmentally friendly than conventional materials [2–7].

The sustainable development concept was consolidated by the World Commission on Environment and Development (WCED) through the Brundtland Report (1987), which refers to considering current needs without compromising future generations in terms of meeting their demands [8]. Discussions on sustainable development have been the main topic of United Nations (UN) member countries' meetings since the 1970s. The UN aims to mitigate anthropic impacts on planet Earth. These discussions have been focused on world population increase, difficulties in access to clean water, urban sanitation, and environmental management, with investments in alternative solid waste management and treatments generated in water treatment plants (WTPs) and wastewater treatment plants (WWTPs) [9]. The deposition of these residues in the environment causes numerous

socio-environmental impacts, such as watercourses silting up, the contamination of soil and urban springs by solid particles and toxic metals, a scarcity of water resources for supply and purification, and mortality in major environmental disasters [10].

The 2030 Agenda published by UN member countries in 2015 addresses the new Sustainable Development Goals (SDGs) at global levels [11,12], as well as ISO 37120 [13], which deals with indicators to assist cities in urban services and the search for sustainability and life quality management. Wastes generated in wastewater treatment and water purification processes are direct by-products of a population's water use, which is essential for maintaining a dignified life and public health. Such basic sanitation infrastructures are essential indicators to guarantee health, cleanliness, life quality, and population dignity [13], which is affirmed in the global SDGs [11].

Geosynthetics have been applied in waste containment systems (WCSs), or geotextile tubes, to dewater wastes [14]. These geosynthetics are structures of woven or non-woven geotextiles or geotextile-related products in bag, container, or tube formats, with their purpose being to receive liquid or semisolid wastes to be filtered [15]. Geosynthetics are polymer-based products that exhibit thermo-visco-elastic-plastic behavior, i.e., the material durability depends on the operating conditions, including the environment, temperature, and different stress conditions (level, rate and duration), among others [16–19]. Compared to traditional techniques (natural and mechanical), WCSs are easier to utilize, lower in cost, and friendlier to the environment. Additionally, they need smaller dewatering areas and consolidation processes and are independent of climate dynamics and electricity, among other things [20,21]. This technique provides a sustainable alternative to dewatering and reduces large waste volumes, such as the waste from WTPs and WWTPs, without impacting the environment of other industrial processes [14].

For example, Fowler et al. [22] and Jiang et al. [23] report the use of geotextile tubes in WWTP waste dewatering. Castro et al. [24] discuss the use of WCSs for dewatering waste collected in septic tanks by vacuum trucks and leachate from landfills as an alternative to the need for sanitation remediation and urban infrastructure due to local population growth. Ruiz and Rendón [25] discuss the use of WCSs as a pioneering application for emptying the oxidation ponds at El Dorado International Airport, Colombia, in 2011, as its operational capacity and imminent expansion had been reached. Guanaes and Sampaio [26] reported WCS use for dewatering WTP waste at a hydroelectric plant construction site in Brazil, serving 15,000 employees.

Furthermore, full-scale WCS applications have been applied to contaminated industrial sediments and mine tailing slurries. For example, Yee et al. [27] presented geotextile tube use for the dewatering of contaminated sediments, which were dredged from a domestic water and industrial wastewater dam. Berg and Oliveira [28] discuss the dewatering of water contaminated by carcinogenic sediments released into the river by paper factories; the results showed around 99% of solids were captured by the WCS. Yang et al. [29] presented the use of geotextile tubes in a phosphate mine in China; Kiffle et al. [30] referred to their use in a gold mine in Canada for dewatering water from the mine's lakes with significant metal levels; and Wilke et al. [31] describe their use in a nickel and zinc mine in Finland that produced large volumes of gypsum slurry as a mining process by-product. Berg and Oliveira [28] report that geotextile tube use was one of the faster remediation measures after the environmental disaster caused by the mining dam rupture in Bento Rodrigues, Brazil, in 2015.

1.2. Cyclic Fatigue in Waste Containment Systems

Geosynthetic durability can be considered the ability to maintain properties throughout the design lifetime under conditions that can alter microstructural and macrostructural properties and compromise the performance of the functions of the material [32–35]. Geosynthetics must be evaluated for each project according to the intended function. The stress to which the materials will be subjected over time should be considered with degra-

dation mechanisms that will compromise the material properties and directly impact the performance of the design functions.

Research to understand geosynthetics' durability is relevant to increasing the reliability of projects with geosynthetics. Thus, direct technical, economic, and environmental gains are obtained with greater design security. An example is the promotion of the partial reduction factor (RF_p) by cyclic loads for the dimensioning of design parameters to guarantee geosynthetic durability [35,36]. Thus, knowledge of the cyclic fatigue loads can improve the reliability of the design lifetime and help predict and prevent large-scale failures [37,38].

Factors that generate cyclic stress should be considered, such as the tensile stress imposed on dewatering systems during filling by pumping and the effects of installation damage, seam strength, weathering degradation conditions, clogging, chemical fluids, and creep [15,33]. Grubb et al. [39,40] report that the exposure of geotextiles to weathering and chemical fluid factors may cause the strain-hardening effect. Measuring the magnitude of retained tensile strength is complex because several isolated and synergistic factors are involved [32].

The literature reports that WCSs are designed to receive more than one pumping cycle and subsequent dewatering to achieve final consolidation. Dewatering and volume reduction are awaited between the pumping cycles carried out until the consolidation phase is reached [41]. The number of pumping cycles depends on different parameters, such as the volumetric capacity of the geotextile tubes, the geotextile tensile strength, and the seams' efficiency [15,18,29,42].

Creep stresses, also called static fatigue, can be incorporated into the design by requiring the final creep strain in dewatering systems to be less than the maximum design value. This requirement ensures that the material has sufficient tensile strength to withstand operating stresses during the filling, dewatering, and solidification of the pumped material stages [15,42]. Therefore, cyclic fatigue should be considered in the design of WCSs under different hydraulic and turbulent loads of the specific process.

Stresses induced during pumping must be supported and dimensioned by geosynthetic mechanical properties, especially tensile strength, with the adoption of partial reduction factors [43]. Leshchinsky et al. [42] discuss using the membrane theory method, which depends on the circumference, height, and maximum tension reached during pumping. These are the circumferential [T_c], axial [T_a], and pumping [T_p] tension. This work emphasizes that such tensions are relieved during the dewatering until the next pumping cycle. Such behavior generates cyclic fatigue requests throughout the process. Depending on the loading levels and the number of cycles, this will reflect the adoption of an additional partial reduction factor. According to Lawson [15], the circumferential tension stresses [T_c] tend to present higher magnitudes during pumping due to the confinement system geometry. The curvature and thickness of the geotextile govern them. The tensions generated in the filling ports of the containment systems are also a function of the pumping pressure, the height reached by the WCS, and the shape of the filling ports.

Mechanical stresses due to cyclic fatigue can also impact the hydraulic parameters of geotextiles, which can compromise the retention capacity of solid particles, as reported in the previous literature [44,45]. For example, Fourie and Addis [46] showed increases in filtration opening in a polypropylene woven geotextile subjected to biaxial tensile loads. Wu et al. [47] reported that when subjecting woven and non-woven geotextiles to uniaxial strain levels, there were increases in filtration openings and flow rates. Palmeira et al. [48] also observed size variations in the filtration opening in non-woven geotextiles under unconfined stresses. Despite the evident influence summarized, this approach is not the scope of this work.

Studies involving applications of monotonic, cyclic, or dynamic tensile load damage were performed to evaluate the use of geosynthetics for reinforcement purposes. Among the parameters considered in the studies, the notable parameters were cyclic loading time, average strain rate, pre-strain, loading frequency, and number of cycles. These studies propose mathematical models based on accelerated laboratory stress–strain tests that can

represent the behavior of geosynthetics under field conditions [19,49–55]. Minster [56] applied the concept of cumulative damage to geosynthetics. Liu and Ling [57] report the possibility of strain hardening, a complex behavior in geosynthetics subjected to cyclic loads. ASTM D 7556 [58] presents methods to determine small-strain tensile properties in geotextiles and geogrids by subjecting samples to cyclic tension.

In waste-dewatering system applications, fatigue cycle parameters may differ from those of geosynthetics evaluated in other studies for reinforcement functions. Therefore, this study is presented to analyze the durability of a geotextile regarding the cyclic fatigue induced, for example, by using dynamic tensile strength tests during the pumping stages in geosynthetic waste-dewatering systems. A polypropylene woven geotextile was used and subjected to cyclic tensile loading levels of 10%, 30% and 50% of the ultimate average tensile strength. The pretension was 0.5% of the ultimate average tensile strength (T_{max}) in the monotonic and cyclic tests. For the parameters obtained during the hysteresis loops, frequency (0.1 Hz), cyclic tensile loading amplitude (10, 30, and 50% of the T_{max}), and number of cycles (10, 20, 30, and 90 cycles) were used. This study contributes to a better understanding of the durability of geotextiles to subsidize decision-making involving designs of sustainable waste-dewatering systems with geosynthetics.

2. Materials and Methods

2.1. Tested Geotextile

The most commonly used polymers in woven geotextiles are polyolefins, i.e., polypropylene and polyethylene, and the polypropylene matrix corresponds to approximately 90% of commercial geotextiles [35,59]. A polypropylene woven geotextile (GTXw) was used to study dynamic fatigue. The objective of this study is not to evaluate the cyclic fatigue durability of different woven geotextiles.

Table 1 shows the properties from the sampling of ten specimens according to the ISO 9862 standard [60]. The number of specimens enables one to obtain the tensile strength results with an expected 2–3% error. The monotonic tensile tests were performed by strip tests [61].

Table 1. Properties of the woven geotextile (GTXw).

Parameters	Standards	Value [3]
Mass per unit area (ρA)	ISO 9864 [62]	271.8 g/m^2 (3.2%)
Thickness (d)	ISO 9863-1 [63]	0.97 mm (5.9%)
Ultimate tensile strength ($T_{\max}$) [1]	ASTM D 5035 [61]	56.2 kN/m (3.6%)
Strain at ultimate tensile ($\epsilon_{\max}$) [1]	ASTM D 5035 [61]	19.2% (4.0%)
Ultimate tensile strength ($T_{\max}$) [2]	ASTM D 5035 [61]	60.6 kN/m (4.9%)
Strain at ultimate tensile ($\epsilon_{\max}$) [2]	ASTM D 5035 [61]	16.9% (4.1%)

[1] Mechanical property in the machine direction (MD). [2] Mechanical property in the cross-machine direction (CMD). [3] The coefficients of variation (COVs) are shown in parentheses.

The choice to use the ASTM D 5035 standard [61] was due to the recognition of the similarity between the results obtained by the ISO 10319 standard [64], for example, in the Dias Filho et al. [65] and Guimarães et al. [66] publications. This standard was used to obtain more specimens: 50 mm wide and 75 mm between the clamps. Therefore, specimens of smaller dimensions allow for obtaining a greater number for the same material sample.

2.2. Cyclic Fatigue Tests

A microprocessed universal mechanical machine with a force capacity of up to 150 kN was used in the cyclic fatigue tensile tests with load control and in a standard atmosphere (20 ± 2 °C at 65 ± 5% relative humidity). Only the 10% and 50% loading levels were investigated for the 90-cycle level. Cyclic fatigue tests were performed on ten specimens for each combination of cyclic tensile loading level and number of cycles. Specimens were obtained in the machine direction (MD).

The maximum load applied (kN) was defined for the cyclic tensile loading levels (Table 2). The setpoint value corresponds to the ultimate average tensile strength (T_{max}) in the machine direction obtained on monotonic tests (56.2 kN/m) according to the ASTM D 5035 standard [61].

Table 2. Definition of forces applied at different loading rates.

Cyclic Tensile Loading Levels (Setpoint) [1]	Number of Cycles	Maximum Load Applied (kN)
10%	10, 20, 30 and 90	0.281
30% [2]	10, 20 and 30	0.843
50%	10, 20, 30 and 90	1.405

[1] Cyclic tensile loading amplitude of ultimate average tensile strength. [2] 90 cycles were not evaluated for a 30% loading level.

Cyclic tensile loading was repeated to reach the maximum controlled setpoint loads. The lower piston returns from the bottom to the initial positioning between jaws (75 mm) with a minimum load equal to the pretension (0.5% of the T_{max}). This is a recommendation of the ASTM D 5035 standard [61] to obtain strain measurements (%). After the total number of cycles for tensile loading levels had been applied, the specimens were tensioned (Figure 1) to determine the ultimate tensile strength (kN/m) and strain (%).

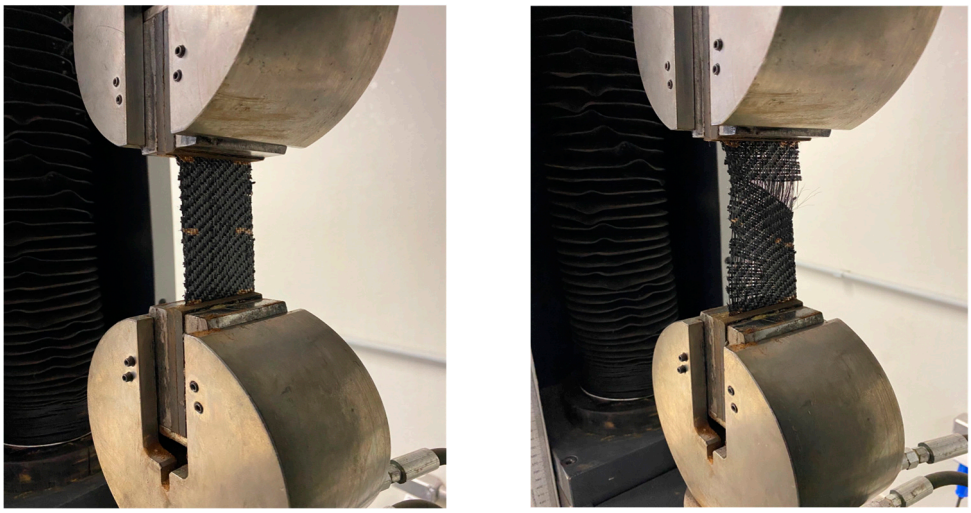

(**a**) (**b**)

Figure 1. Cyclic fatigue tests: (**a**) Initial conditions; (**b**) Specimens tensioned after application of the fatigue stress.

The experimental data were statistically analyzed. Box plots were constructed to represent the variation in the sample data. The results were compared with the tensile strength of the intact geotextile to obtain the population mean by confidence intervals (CIs) at a 95% confidence level. These intervals were constructed based on Student's t distribution since the material follows a normal distribution [67] and the population standard deviation is unknown [68]. The mathematical model that best describes the tensile strength (%) was obtained as a function of the loading levels and number of cycles for the study conditions. Mathematical models are an important tool for understanding the material durability behavior caused by factors that can induce their degradation [17].

The authors emphasize that the investigated conditions represent the application of woven geotextiles for use in WCSs and simulate the filling, dewatering, and consolidation stages [15]. Furthermore, the difference in ultimate tensile strength of the tested geotextile obtained by monotonic and cyclic load tests was investigated by statistical analysis.

3. Results and Discussion

3.1. Statistical Analyses of Cyclic Fatigue Tests

3.1.1. Box Plot Analyses

Table 3 summarizes the cyclic fatigue test results that are used to complement the graphical analysis by box plot (Figure 2). Figure 2 shows that for a tensile loading level of 10%, only the application of 10 cycles induced a representative change in the tensile strength of the geotextile. The mean value obtained (62.3 kN/m) is above the interquartile range of the intact sample, which indicates an increase of 10.8% in tensile strength and a greater deformation than the mean value of the intact sample. As Ashmawy and Bourdeau [50] argued, the redistribution of stresses to undamaged fibers during hysteresis loops can explain this behavior. This phenomenon is known as strain hardening [57].

Table 3. Cyclic fatigue test results.

Number of Cycles	Cyclic Tensile Loading Levels (Setpoint)	Parameters [1]		Tensile Strength Loss (%)	Partial Reduction Factor (RFp) [2]
		T_{max} (kN/m)	ϵ_{max} (%)		
10 cycles	10%	62.3 (1.5%)	20.0 (2.0%)	NA	1.0
	30%	55.7 (3.8%)	19.6 (5.3%)	0.9	1.0
	50%	51.9 (6.3%)	18.8 (6.9%)	7.7	1.1
20 cycles	10%	56.7 (2.7%)	19.9 (2.9%)	0	1.0
	30%	53.7 (3.5%)	18.6 (5.8%)	4.4	1.0
	50%	52.1 (4.6%)	19.3 (10.0%)	7.3	1.1
30 cycles	10%	55.7 (8.6%)	18.8 (8.8%)	0.9	1.0
	30%	54.0 (2.4%)	19.2 (3.6%)	3.9	1.0
	50%	52.9 (8.6%)	17.4 (4.9%)	5.9	1.1
90 cycles	10%	54.1 (3.3%)	18.7 (4.8%)	3.7	1.0
	30%	N/A	N/A	N/A	N/A
	50%	47.9 (23.8%)	15.7 (25.1%)	14.8	1.2

[1] The coefficients of variation (COVs) are shown in parentheses. [2] Partial reduction factors for the tensile strength after cyclic loading.

The specimens that were submitted to 20 cycles (tensile loading level of 10%) exhibited a small increment in strain compared to the intact sample. No representative changes in tensile strength were observed, and only the first quartile was within the interquartile range of the intact geotextile. In the 30-cycle situation, the tensile and strain values are within the interquartile range but with greater data dispersion. The 90 cycles generated a tensile strength loss of 3.8%, and only the third quartile is contained in the interquartile range; a similar situation was observed for the strain.

The tensile strength and strain results at the 30% cyclic loading level (10 cycles) are within the interquartile range but with greater data dispersion. The application of 20 and 30 cycles demonstrates a similar loss of tensile strength, which was analyzed in terms of mean values and coefficient of variation (COV).

Increasing the loading level to 50% decreases the tensile strength (10 and 20 cycles). Regarding strain, the sample values are within the interquartile range and similar when analyzing the average results and respective COV (Table 3). For 30 cycles, although there was a minor loss of tensile strength (5.9%), the results showed a greater dispersion. Sample results were below the interquartile range for strain results. Higher tensile strength loss and strain were observed for 90 cycles, with a significant increase in the dispersion of the sample results.

Regarding the partial reduction factors obtained (Table 3), Leshchinsky et al. [42] recommend the application of an RF_p for installation damage, which may be associated with an accidental increase in waste pumping pressure at a minimum value of 1.3.

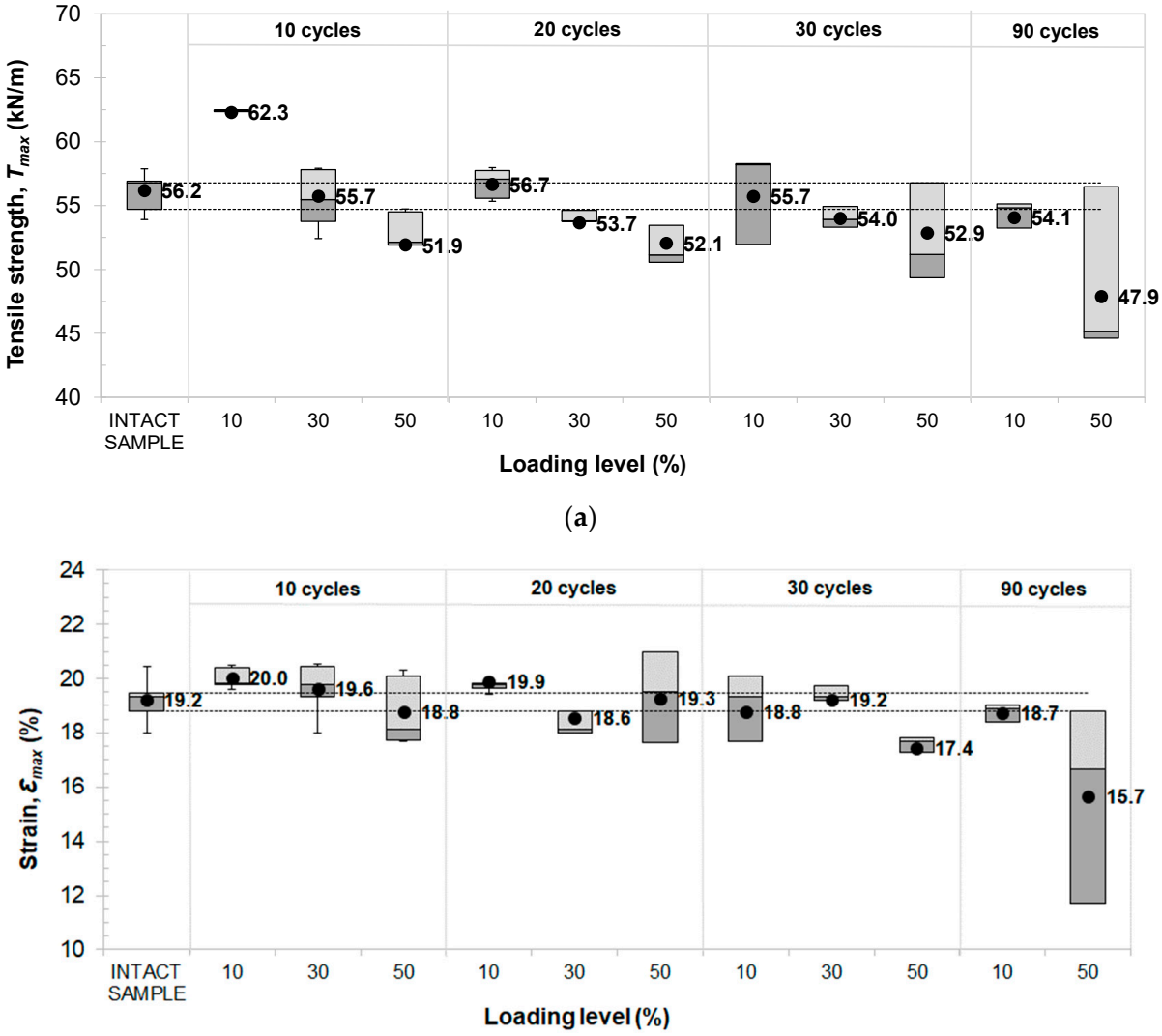

Figure 2. Box plot analyses under cyclic tensile loading levels: (**a**) Tensile strength under loading level; (**b**) Strain under loading level.

3.1.2. Confidence Interval Analyses

Figure 3 graphically shows the CIs at a 95% confidence level for the different investigated cases. The populational average (μ) shows that the tensile strength of the cyclic fatigue tests is shifted to the left of the CI for the intact sample ($54.8 < \mu < 57.5$ kN/m), except for 10 cycles (10% and 20% of the loading levels) and 20 cycles (10% loading level). The average populational behavior resembles the sample mean (Figure 2). In addition, the CIs indicate an increase in the dispersion of the results when the number of cycles and tensile loading levels increase, except for the 10% loading level (10 cycles). Cyclic tensile loadings show distinct changes in the tensile strength of the geotextile (populational parameter) as a function of the analyzed conditions, which can affect the geotextile durability.

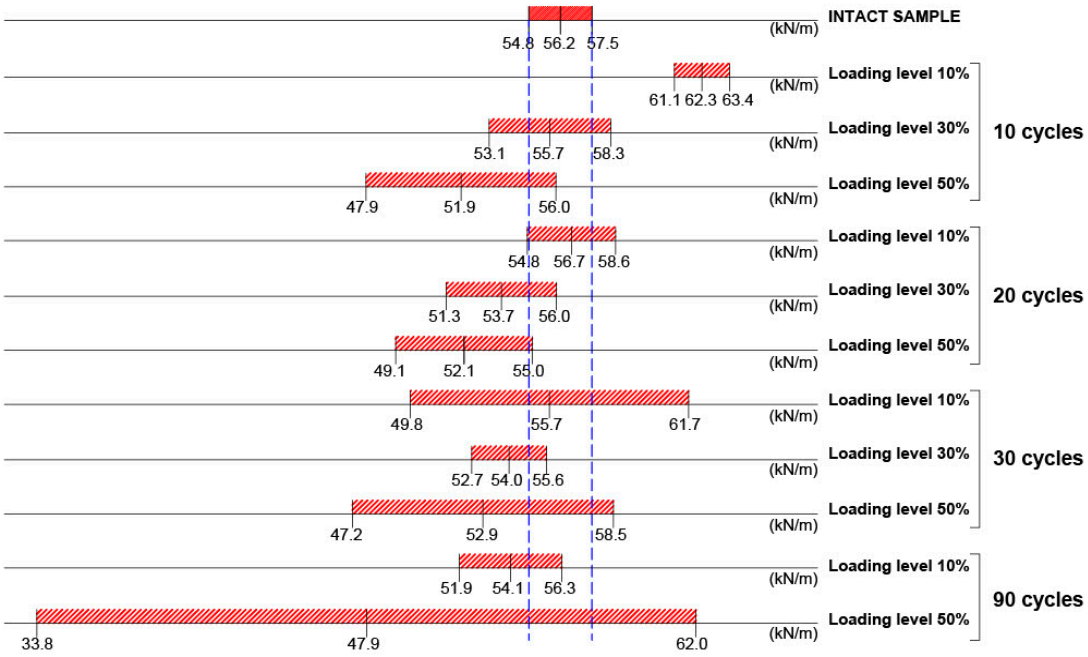

Figure 3. Confidence interval (CI), with a 95% confidence level, for geotextile subjected to fatigue tests (ten specimens for each loading level and number of cycles).

3.2. Tensile Strength in Monotonic and Cyclic Fatigue Tests

Figure 4 shows tensile strength (kN/m) versus strain (%) curves obtained for 10, 20, 30, and 90 cycles over the applied loading levels (10%, 30%, and 50%).

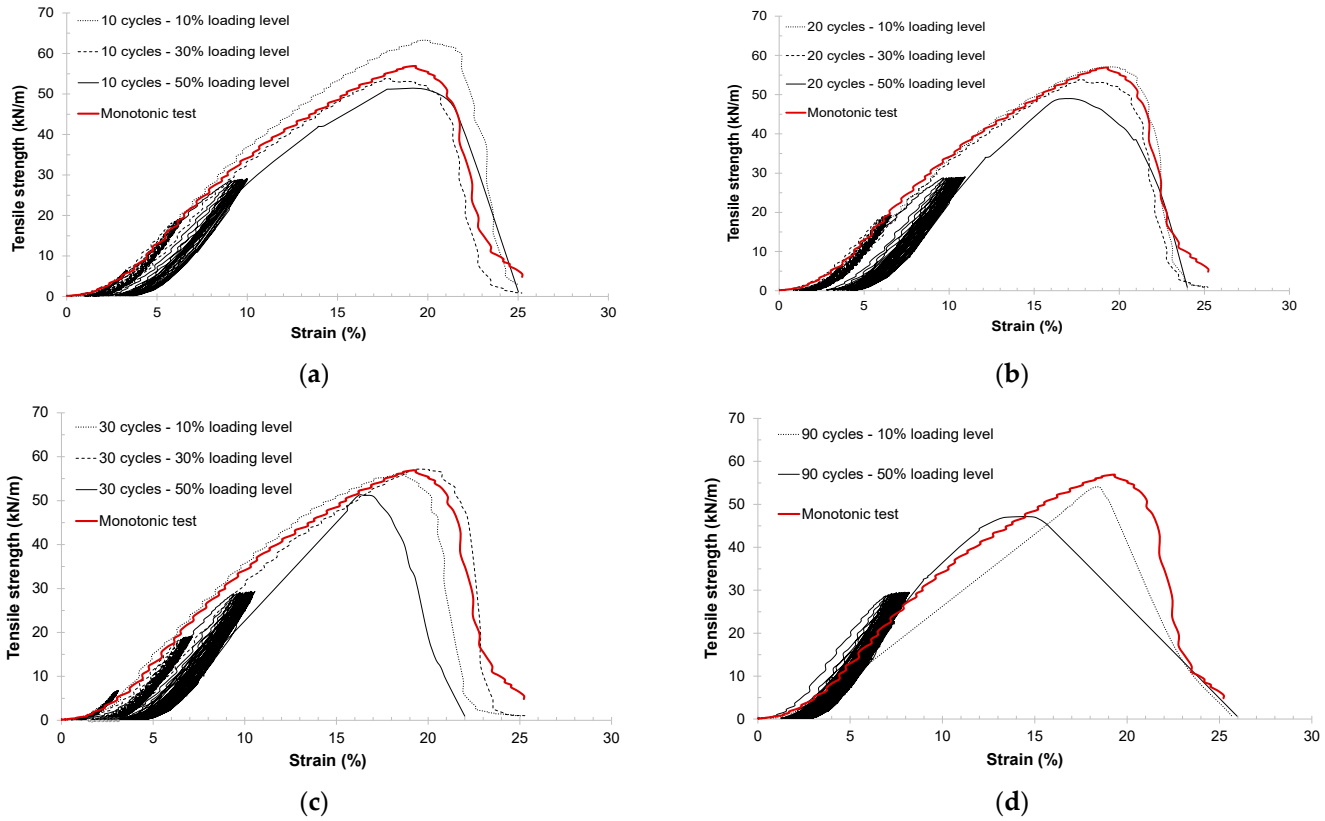

Figure 4. Tensile strength (kN/m) versus strain (%) curves in monotonic and cyclic tests at f = 0.1 Hz: (**a**) 10 cycles; (**b**) 20 cycles; (**c**) 30 cycles; (**d**) 90 cycles.

Compared to the monotonic behavior curve of the polypropylene GTXw, there is a decrease in the T_{max} with increased cyclic fatigue numbers and applied loading levels. We highlight the reduction in the T_{max} obtained for the loading level of 50% and 90 cycles (Figure 4d), except for the behavior observed for 10 cycles and a loading level of 10%, where the strain hardening phenomenon occurred (Figure 4a).

3.3. Hysteretic Stiffness under Cyclic Fatigue Tests

Figure 5 shows hysteretic stiffness results (J_h, kN/m) obtained under cyclic fatigue loads. There are slight increases in J_h for the same loading level as the number of cycles increases. This behavior was more pronounced for the 50% loading level. Figure 6 represents the response surface of parameter J_h as a function of variables (loading level and number of cycles), supporting the behavior shown in Figure 5.

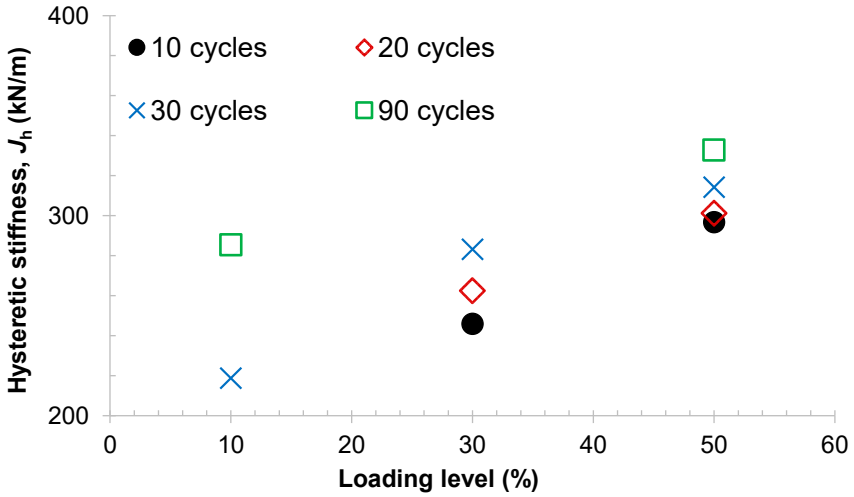

Figure 5. Hysteretic stiffness (J_h) for loading levels.

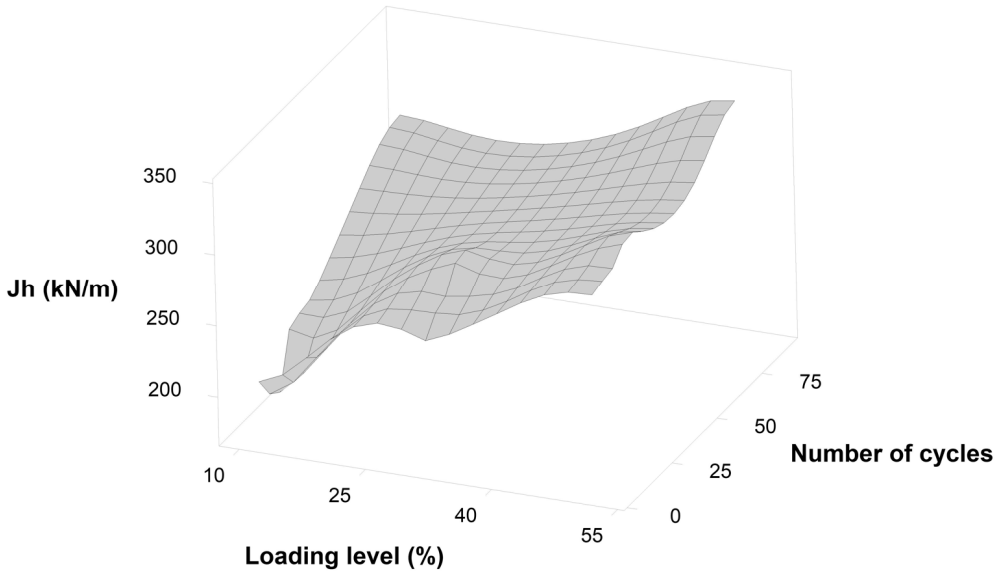

Figure 6. Response surface under cyclic fatigue tests for hysteretic stiffness (J_h).

3.4. Mathematical Model for the Behavior of Woven Geotextile Using Cyclic Fatigue Tests

Figure 7 shows mathematical models based on the monotonic and cyclic fatigue results for the analyzed cycles (10, 20, and 30 cycles), represented by exponential functions, to estimate the T_{max} for each loading level (10%, 30%, and 50%). Models fit an exponential

function (R^2 greater than 97%), where the y-axis is the ultimate tensile strength (kN/m) as a function of the loading levels applied (%) per number of cycles, according to Equation (1).

$$R = Ke^{-(Y).x} \quad (1)$$

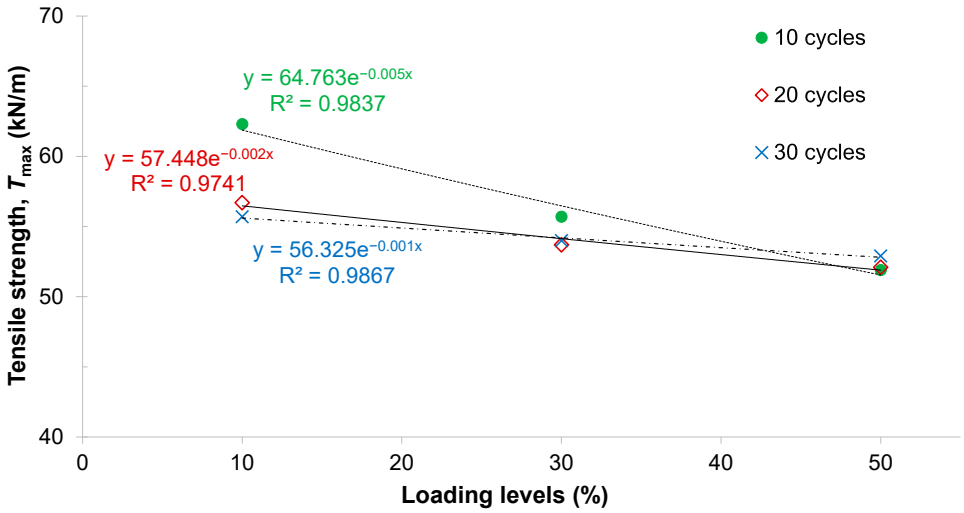

Figure 7. Mathematical models for cyclic fatigue tests.

In the equations above, R is the ultimate tensile strength (kN/m); K is the coefficient dependent on the tensile strength characteristics of the intact geotextile (kN/m) as the mean value; x is the loading level (%); and Y is the exponent equal to 10^{-3}, dependent on the synergism of the factors analyzed (in other words, the number of cycles and loading levels).

For the loading level of 10% and 10 cycles, the coefficient K (Equation (1)) reflects the strain-hardening phenomenon in this situation. For the other exponential mathematical models obtained (20 and 30 cycles), the K coefficient is found in the CI lower and upper limits (see Figure 3), with a confidence level of 95%, for a woven geotextile sample.

Specimens subjected to a loading level of 30% and 10 cycles showed a retained tensile strength close to the intact material, while for 20 and 30 cycles, the ultimate tensile strengths retained (kN/m) were similar. The retained tensile strength results obtained were also close for the 50% loading level application to 10 and 20 cycles. The authors emphasize that at 30 cycles, although the average retained strength is higher than the values observed for 10 and 20 cycles, the dispersion of these data (Figure 2) is highlighted. With 50% loading level application to 90 cycles, the tensile strength loss is 14.8%, and the dispersion of the sample (Figure 2) and population (Figure 3) data is highlighted. These data were not shown in Figure 7 due to performing 90 cycles only for 10% and 50% loading levels.

The response surface in Figure 8 shows that both factors (number of cycles and loading level) influence the ultimate tensile strength (T_{max}) for the evaluated conditions and a frequency of 0.1 Hz. The 10% loading level application presented strain hardening for 10 cycles (62.3 kN/m). A loading level of 50% reduced T_{max} as the number of cycles increased. This behavior was more evident for 90 cycles, resulting in a partial reduction factor (RF_p) of 1.2. This behavior did not occur for the other loading levels (Table 3).

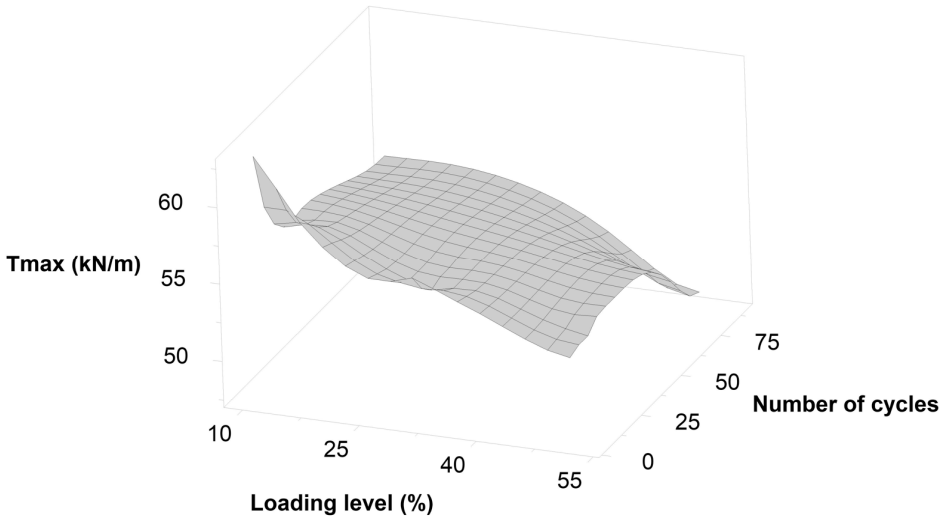

Figure 8. Response surface under cyclic fatigue tests for ultimate tensile strength (T_{max}).

4. Conclusions

This study focuses on the analysis of tensile-strain and hysteretic stiffness behaviors using cyclic loads in accelerated tests, seeking to contribute to a better understanding of the behavior of field conditions in dewatering systems. With tensile loading levels of 10% and 10 cycles, the polypropylene woven geotextile in this study presented an increase in tensile strength due to strain hardening under the analyzed conditions. Regarding hysteretic stiffness, there is a slight increase for the same loading level as the number of cycles increases. This behavior was more pronounced for the 50% loading level. Changes observed for a 50% loading level and 90 cycles are noteworthy, with a decrease of 14.8% in tensile strength due to cyclic fatigue and implied an RF_p of 1.2. Geotextiles are subjected to multiple conditions for use in waste-dewatering systems. Therefore, it is necessary to consider other partial reduction factors, such as installation damage, creep, seam strength, weathering, chemical fluids, and clogging, related to site requirements. Obtaining the mathematical models represented by exponential functions can be promising for understanding geosynthetic durability under different factor conditions. Further studies are needed to evaluate cyclic fatigue conditions in woven and non-woven geotextiles from other polymeric matrices.

Author Contributions: Conceptualization, M.G.A.G., P.V.G.d.O., D.d.C.U. and E.L.P.; Methodology, P.V.G.d.O. and D.d.C.U.; Validation, M.G.A.G., P.V.G.d.O. and D.d.C.U.; Formal analysis, M.G.A.G., D.d.C.U. and B.M.C.U.; Investigation, P.V.G.d.O., D.d.C.U. and E.L.P., Resources: P.V.G.d.O. and D.d.C.U.; Writing-Review and Editing, M.G.A.G., D.d.C.U. and B.M.C.U. All authors have read and agreed to the published version of the manuscript.

Funding: This research received no external funding.

Institutional Review Board Statement: Not applicable.

Informed Consent Statement: Not applicable.

Data Availability Statement: Publicly available datasets were analyzed in this study. This data can be found here: http://www.repositorio.ufop.br/jspui/handle/123456789/13783 (accessed on 11 September 2023).

Acknowledgments: The authors would like to acknowledge the Federal University of Ouro Preto (NUGEO/EM/UFOP) and the Federal Center of Technological Education of Minas Gerais (CEFET-MG) for the support. Huesker is also acknowledged for providing the geotextile.

Conflicts of Interest: The authors declare no conflict of interest.

Nomenclature

ρA	Mass per unit area (kg/m^2)
μ	Populational average (kN/m)
d	Thickness (m)
T_{max}	Ultimate tensile strength (kN/m)
ϵ_{max}	Strain at ultimate tensile (%)
GTXw	Woven geotextile
J_h	Hysteretic stiffness
R^2	Coefficient of determination (dimensionless)
RF_p	Partial reduction factor
CIs	Confidence Intervals
UN	United Nations
WCDE	World Commission on Environment and Development
WCSs	Waste Containment Systems
WTPs	Water Treatment Plants
WWTPs	Wastewater Treatment Plants

References

1. Biermann, F. The future of 'environmental' policy in the Anthropocene: Time for a paradigm shirf. *Environ. Polit.* **2021**, *30*, 61–80. [CrossRef]
2. Dixon, N.; Fowmes, G.; Frost, M. Global challenges, geosynthetics solutions and counting carbon. *Geosynth. Int.* **2017**, *24*, 451–464. [CrossRef]
3. Palmeira, E.M.; Araújo, G.L.S.; Santos, E.C.G. Sustainable solutions with geosynthetics and alternative construction materials—A review. *Sustainability* **2021**, *13*, 12756. [CrossRef]
4. Rimoldi, P.; Shamrock, J.; Kawalec, J.; Touze, N. Sustainable use of geosynthetics in dykes. *Sustainability* **2021**, *13*, 4445. [CrossRef]
5. Touze, N. Healing the world: A geosynthetics solution. *Geosynth. Int.* **2021**, *28*, 1–31. [CrossRef]
6. Tseng, I.-F.; Hsu, C.-H.; Cheng, H.-C.; Chen, Y.-S. Application of geotextile tubes to coastal silt mitigation: A case study in Niaoyu Fishing Harbor. *Sustainability* **2023**, *15*, 32024. [CrossRef]
7. Dabrowska, J.; Kiersnowska, A.; Zieba, Z.; Trach, Y. Sustainability of geosynthetics-based solutions. *Environments* **2023**, *10*, 64. [CrossRef]
8. United Nations World Commission on Environment and Development. *Report of the World Commission on Environment and Development: Our Common Future*; Oxford University Press: Oxford, UK, 1987; 300p.
9. Le, P.G.; Le, H.A.; Dinh, X.T.; Nguyen, K.L.P. Development of sustainability assessment criteria in selection of municipal solid waste treatment technology in developing countries: A case of Ho Chi Minh City, Vietnam. *Sustainability* **2023**, *15*, 7917. [CrossRef]
10. Yee, T.W.; Lawson, C.R. Modelling the geotextile tube dewatering process. *Geosynth. Int.* **2012**, *19*, 339–353. [CrossRef]
11. United Nations. *Transforming Our World: The 2030 Agenda for Sustainable Development. Document A/RES/70/1*; UN: New York, NY, USA, 2015.
12. Baste, I.A.; Watson, R.T. Tackling the climate, biodiversity and pollution emergencies by making peace with nature 50 years after the Stockholm Conference. *Glob. Environ. Chang.* **2022**, *73*, 102466. [CrossRef]
13. *ISO 37120:2018*; Sustainable Cities and Communities—Indicators for City Services and Quality of Life. International Organization for Standardization: Geneva, Switzerland, 2018.
14. Fowler, J.; Duke, M.; Schmidt, M.L.; Crabtree, B.; Bagbby, R.M.; Etrainer, E. Dewatering sewage sludge and hazardous sludge with geotextile tubes. In Proceedings of the 7th International Conference on Geosynthetics, 7ICG, Nice, France, 22–27 September 2002.
15. Lawson, C.R. Geotextile containment for hydraulic and environmental engineering. *Geosynth. Int.* **2008**, *15*, 384–427. [CrossRef]
16. Perkins, S.W. Constitutive modeling of geosynthetics. *Geotext. Geomembr.* **2000**, *18*, 273–292. [CrossRef]
17. Maxwell, A.S.; Broughton, W.R.; Dean, G.; Sims, G.D. *Review of Accelerated Ageing Methods and Lifetime Prediction Techniques for Polymeric Materials*; NPL Report DEPC MPR 016; National Physical Laboratory: Teddington, UK, 2005; 84p.
18. Allen, S.R. Geotextile durability. In *Geotextiles: From Design to Applications*; Koerner, R.M., Ed.; Woodhead Publishing: Cambridge, UK, 2016; pp. 177–215.
19. Cardile, G.; Moraci, N.; Pisano, M. Tensile behaviour of an HDPE geogrid under cyclic loading: Experimental results and empirical modelling. *Geosynth. Int.* **2017**, *24*, 95–112. [CrossRef]
20. Ardila, M.A.A.; Souza, S.T.; Silva, J.L.; Valentin, C.A.; Dantas, A.D.B. Geotextile tube dewatering performance assessment: An experimental study of sludge dewatering generated at a water treatment plant. *Sustainability* **2020**, *12*, 98129. [CrossRef]
21. Guimarães, M.G.A.; Urashima, D.C.; Vidal, D.M. Dewatering of sludge from a water treatment plant in geotextile closed systems. *Geosynth. Int.* **2014**, *21*, 310–320. [CrossRef]
22. Fowler, J.; Larkins, K.; Duke, M.L. *Dredging Aerobic Digested Biosolids into Geotextile Tubes for Dewatering*; New Orleans East Municipal Sewage Treatment Plant: New Orleans, LA, USA, 2005.

23. Jiang, Y.; Liu, Z.; Cui, M.; Su, R.; Liu, Z.; Zhang, J.; Huang, R. Risk Assessment and treatment of the heavy metals contaminated sediments via stabilisation and dewatering in geotextile tubes. *Chem. Eng. Trans.* **2020**, *81*, 241–246. [CrossRef]
24. Castro, N.P.B.; Melo, L.C.Q.C.; Escobar, L.G.B. Environmental integrated solution for septic tank sludge and landfill leachate using geotextile tubes dewatering technology. In Proceedings of the First Pan American Geosynthetics Conference & Exhibition, GeoAmericas 2008, Cancun, Mexico, 2–5 March 2008.
25. Ruiz, N.R.; Rendón, M. Geotextile tubes in sludge confinement and dewatering applications at Eldorado International Airport. In Proceedings of the Second Pan American Geosynthetics Conference & Exhibition, GeoAmericas 2012, Lima, Peru, 6–9 May 2012.
26. Guanaes, E.A.; Sampaio, D.V. Recent applications of geotextile tubes for sludge and slurry dewatering—Brazil. In Proceedings of the Second Pan American Geosynthetics Conference & Exhibition, GeoAmericas 2012, Lima, Peru, 6–9 May 2012.
27. Yee, T.W.; Lawson, C.R.; Wang, Z.Y.; Ding, L.; Liu, Y. Geotextile tube dewatering of contaminated sediments, Tianjin Eco-City, China. *Geotext. Geomembr.* **2012**, *31*, 39–50. [CrossRef]
28. Berg, G.V.D.; Oliveira, F.A.P. Adequacy of geotextile tube dewatering in three river remediation scenarios. *WIT Trans. Ecol. Environ.* **2019**, *234*, 155–165. [CrossRef]
29. Yang, Y.; Wei, Z.; Cao, G.; Yang, Y.; Wang, H.; Zhuang, S. A case study on utilizing geotextile tubes for tailings dams construction in China. *Geotext. Geomembr.* **2019**, *47*, 187–192. [CrossRef]
30. Kiffle, Z.B.; Bhatia, S.K.; Lebster, G.E. Dewatering of mine tailing slurries using geotextile tube: Case histories. *Int. J. Geosynth. Ground Eng.* **2023**, *9*, 10. [CrossRef]
31. Wilke, M.; Breytenbach, M.; Reunanen, J.; Hilla, V.M. Efficient and environmentally sustainable tailings treatment and storage by geosynthetic dewatering tubes: Working principles and Talvivaara case study. In Proceedings of the Tailings and Mine Waste, Vancouver, BC, Canada, 26–28 October 2015.
32. Lopes, M.P.; Lopes, M.L. *The Durability of Geosynthetics*; FEUP Edições: Porto, Portugal, 2010; 294p. (In Portuguese)
33. Greenwood, J.H.; Schroeder, H.F.; Voskamp, W. *Durability of Geosynthetics*; CUR Committee C 187-Building & Infrastructure: Gouda, The Netherlands, 2012; 295p.
34. *ASTM D 5819:2022*; Standard Guide for Selectiong Test Methods for Experimental Evaluation of Geosynthetics Durability. American Society for Testing and Materials. ASTM International: West Conshohocken, PA, USA, 2022.
35. *ISO/TS 13434:2020*; Geosynthetics: Guidelines for the Assessment of Durability. International Organization for Standardization: Geneva, Switzerland, 2020.
36. Bezuijen, A.; Vastenburg, E.W. *Design Rules and Applications*; CRC Press: Deltares, MD, USA, 2013; 166p.
37. Vieira, C.S.; Lopes, M.L. Effects of the loading rate and cyclic loading on the strength and deformation properties of a geosynthetics. *Constr. Build. Mater.* **2013**, *49*, 758–765. [CrossRef]
38. Perkins, S.W.; Haselton, H.N. Resilient response of geosynthetics from cyclic and sustained in-air tensile loading. *Geosynth. Int.* **2019**, *26*, 428–435. [CrossRef]
39. Grubb, D.G.; Diesing, W.E., III; Cheng, S.C.J.; Sabanas, R.M. Comparison of geotextile durability to outdoor exposure conditions in the Peruvian Andes and Southeastern USA. *Geosynth. Int.* **2000**, *7*, 23–45. [CrossRef]
40. Grubb, D.G.; Diesing, W.E., III; Cheng, S.C.J.; Sabanas, R.M. Comparison of the durability of geotextiles in an alkaline mine tailings environment. *Geosynth. Int.* **2001**, *8*, 49–80. [CrossRef]
41. Barrentes, M.A.V.; Ribeiro, L.F.M.; Palmeira, E.M. Influence of the filling process on the behaviour of geotextile tubes. *Soils Rock.* **2023**, *46*, e2023010522. [CrossRef]
42. Leshchinsky, D.; Leshchinsky, O.; Ling, H.I.; Gilbert, P.A. Geosynthetic Tubes for Confining Pressurized Slurry: Some Design Aspects. *J. Geotech. Geoenviron.* **1996**, *122*, 682–690. [CrossRef]
43. Assinder, P.J.; Breytenbach, M.; Wiemers, J.; Hortkorn, F. Utilizing geotextile tubes to extend the life of a Tailings Storage Facility. In Proceedings of the First South African Geotechnical Conference, Sun City, South Africa, 5–6 May 2016.
44. Cooke, T.; Rebenfeld, L. Effect of Chemical composition and physical structure of geotextiles on their durability. *Geotext. Geomembr.* **1988**, *7*, 7–22. [CrossRef]
45. Fourie, A.B.; Kuchena, S.M. The influence of tensile stresses on the filtration characteristics of geotextiles. *Geosynth. Int.* **1995**, *2*, 455–471. [CrossRef]
46. Fourie, A.B.; Addis, P.C. Changes in filtration opening size of woven geotextiles subjected to tensile loads. *Geotext. Geomembr.* **1999**, *17*, 331–340. [CrossRef]
47. Wu, C.S.; Hong, Y.S.; Wang, R.H. The influence of uniaxial tensile strain on the pore size and filtration characteristics of geotextiles. *Geotext. Geomembr.* **2008**, *26*, 250–262. [CrossRef]
48. Palmeira, E.M.; Melo, D.L.A.; Moraes-Filho, I.P. Geotextile filtration opening size under tension and confinement. *Geotext. Geomembr.* **2019**, *47*, 566–576. [CrossRef]
49. Bathurst, R.J.; Cai, Z. In-isolation cyclic load-extension behaviour of two geogrids. *Geosynth. Int.* **1994**, *1*, 1–19. [CrossRef]
50. Ashmawy, A.K.; Bourdeau, P.L. Response of a woven and a nonwoven geotextile to monotonic and cyclic simple tension. *Geosynth. Int.* **1996**, *3*, 496–515. [CrossRef]
51. Kongkitkul, W.; Hirakawa, D.; Tatsuoka, F.; Uchimura, T. Viscous deformation of geosynthetic reinforcement under cyclic loading conditions and its model simulation. *Geosynth. Int.* **2004**, *11*, 73–99. [CrossRef]
52. Moraci, N.; Cardile, G. Influence of cyclic tensile loading on pullout resistance of geogrids embedded in a compacted granular soil. *Geotext. Geomembr.* **2009**, *27*, 475–487. [CrossRef]

53. Zanzinger, H.; Hangen, H.; Alexiew, D. Fatigue behaviour of a PET-Geogrid under cyclic loading. *Geotext. Geomembr.* **2010**, *28*, 251–261. [CrossRef]
54. Leonardi, G.; Lo Bosco, D.; Palamara, R.; Suraci, F. Finite element analysis of geogrid-stabilized unpaved roads. *Sustainability* **2020**, *12*, 51929. [CrossRef]
55. Leonardi, G.; Suraci, F. A 3D-FE model for the rutting prediction in geogrid reinforced flexible pavements. *Sustainability* **2022**, *14*, 63695. [CrossRef]
56. Minster, J. Prediction of long-term geosynthetic strength using cumulative damage theory. *Geotext. Geomembr.* **1986**, *3*, 77–88. [CrossRef]
57. Liu, H.; Ling, H.I. Modeling cyclic behavior of geosynthetics using mathematical functions: Masing rule and bounding surface plasticity. *Geosynth. Int.* **2006**, *13*, 234–245. [CrossRef]
58. *ASTM D 7556:2019*; Standard Test Methods for Determing Small-Strain Tensile Properties of Geogrids and Geotextiles by In-Air Cyclic Tension Tests. American Society for Testing and Materials, ASTM International: West Conshohocken, PA, USA, 2019.
59. Koerner, R.M. *Designing with Geosynthetics*, 6th ed.; Xlibris Corporation: Bloomington, IN, USA, 2012; Volume 1, 526p.
60. *ISO 9862:2005*; Geosynthetics—Sampling and Preparation of Test Specimens. International Organization for Standardization: Geneva, Switzerland, 2005.
61. *ASTM D 5035:2019*; Standard Test Method for Breaking Force and Elongation of Textile Fabrics (Strip Method). American Society for Testing and Materials, ASTM International: West Conshohocken, PA, USA, 2019.
62. *ISO 9864:2005*; Geosynthetics—Test Method for the Determination of Mass per Unit Area of Geotextiles and Geotextile-Related Products. International Organization for Standardization: Geneva, Switzerland, 2005.
63. *ISO 9863-1:2016*; Geosynthetics—Determination of Thickness at Specified Pressures—Part 1: Single Layers. International Organization for Standardization: Geneva, Switzerland, 2016.
64. *ISO 10319:2015*; Geosynthetics: Wide-Width Tensile Test. International Organization for Standardization: Geneva, Switzerland, 2015.
65. Dias Filho, J.L.E.; Maia, P.C.A.; Xavier, G.C. A short-term model for extrapolating unconfined creep deformation data for woven geotextiles. *Geotext. Geomembr.* **2019**, *47*, 792–797. [CrossRef]
66. Guimarães, M.G.A.; Vidal, D.M.; Urashima, D.C.; Castro, C.A.C. Degradation of polypropylene woven geotextile: Tensile creep and weathering. *Geosynth. Int.* **2017**, *24*, 213–223. [CrossRef]
67. Urashima, B.M.C. Methodology for Determining the Failure Probability during the Geosynthetics' Projects Service Life. Master's Thesis, Master in Geotechnics, Federal University of Ouro Preto (NUGEO/EM/UFOP), Ouro Preto, Brazil, 30 May 2022. (In Portuguese).
68. Montgomery, D.C. *Design and Analysis of Experiments*, 7th ed.; John Wiley & Sons Inc.: New York, NY, USA, 2008; 680p.